Towards forecasting volcanic eruptions using seismic noise

FLORENT BRENGUIER[1,2]*, NIKOLAI M. SHAPIRO[2], MICHEL CAMPILLO[1], VALÉRIE FERRAZZINI[3], ZACHARIE DUPUTEL[3], OLIVIER COUTANT[1] AND ALEXANDRE NERCESSIAN[2]

[1]Laboratoire de Géophysique Interne et de Tectonophysique, CNRS & Univ. Joseph Fourier, Grenoble, France
[2]Laboratoire de Sismologie, Institut de Physique du Globe de Paris, CNRS, Paris, France
[3]Observatoire Volcanologique du Piton de la Fournaise, IPGP, La Réunion, France
*e-mail: fbrengui@ipgp.jussieu.fr

Published online: 20 January 2008; doi:10.1038/ngeo104

Volcanic eruptions are preceded by increased magma pressures, leading to the inflation of volcanic edifices[1]. Ground deformation resulting from volcano inflation can be revealed by various techniques such as spaceborne radar interferometry[2], or by strain- and tiltmeters[3]. Monitoring this process in real time can provide us with useful information to forecast volcanic eruptions. In some cases, however, volcano inflation can be localized at depth with no measurable effects at the surface, and despite considerable effort[4,5] monitoring changes in volcanic interiors has proven to be difficult. Here we use the properties of ambient seismic noise recorded over an 18-month interval to show that changes in the interior of the Piton de la Fournaise volcano can be monitored continuously by measuring very small relative seismic-velocity perturbations, of the order of 0.05%. Decreases in seismic velocity a few weeks before eruptions suggest pre-eruptive inflation of the volcanic edifice, probably due to increased magma pressure. The ability to record the inflation of volcanic edifices in this fashion should improve our ability to forecast eruptions and their intensity and potential environmental impact.

Volcanoes are among the most dynamic geological entities, and their eruptions provide a dramatic manifestation of the Earth's internal activity. However, strong eruptions are only short episodes in the history of volcanoes, which remain quiescent most of the time. During these inter-eruption periods, slow processes such as changes in the magma supply to the reservoir and changes in the physical or chemical properties of magma lead to perturbations of the reservoir pressure and thus prime the volcano for a new eruption. It is, therefore, very important to better describe these processes to fully understand the functioning of active magmatic systems and to improve our ability to forecast volcanic eruptions.

The inter-eruptive magma pressurization and/or intrusions of dykes result in subtle changes in the shape of the volcanic edifices that may be detected by modern strainmeters and tiltmeters[3]or by satellites[2]. The main limitation of these geodetic methods is that they are based on the interpretation of displacements or tilts observed near the surface, which limits their sensitivity to changes located at depth. Volcanic seismicity provides information about short-term (few seconds to few days) mechanical processes occurring within volcanoes at depth. The spatio-temporal evolution of magma migration can be retrieved by precise location of seismic events[6] and by accurate determination of seismic source properties[7,8]. However, analysis of volcanic seismicity cannot be used to detect the aseismic magma pressurization preceding fracturing and magma migration. The inter-eruptive processes also produce perturbations of the elastic properties of volcanic edifices. They can be detected as changes in the travel times of seismic waves propagating within the volcanic edifices by using coda waves from repetitive seismic sources such as multiplets[4,9,10] or small summital volcanic explosions[5,11] or correlations of a diffuse seismic wavefield excited by long-period seismo-volcanic events[12]. However, these methods on the basis of seismo-volcanic sources do not provide information about time periods when volcanoes are seismically quiescent. More recently, repeated seismic tomographies[13] have been used to detect seismic velocity variations within Mount Etna over periods of a few years. This method reveals variations of the internal volcanic structure before and after an eruption. However, the construction of repetitive tomographic images requires long time periods of observation of seismicity and cannot be done continuously. Moreover, the accuracy of repetitive tomographies is limited and may be insufficient to detect small velocity variations (less than 1%) associated with magma pressurization processes.

In this paper, we go beyond the limitations of methods on the basis of seismo-volcanic sources by recovering temporal velocity variations within the Piton de la Fournaise volcano using continuous ambient seismic noise records. The basic idea is that a cross-correlation of random seismic wavefields such as coda or noise recorded at two receivers yields the Green function, that is, the impulse response of the medium at one receiver as if there were a source at the other[14–18]. This property has been used for imaging the crust at regional scales[19,20] and, more recently, has been applied to infer the internal structure of the Piton de la Fournaise volcano at La Réunion island[21]. By computing noise cross-correlations between different receiver pairs for consecutive time periods, we make each receiver act as a virtual highly repetitive seismic source. The associated reconstructed seismic waves (Green functions) can then be used to detect temporal perturbations associated with small velocity changes[22,23] (less than 1%).

We applied this method to study the Piton de la Fournaise volcano on La Réunion island (Fig. 1a). During the past two centuries the average time between consecutive eruptions of this volcano has been about 10 months[24]. Geodetic and seismic data suggest that the Piton de la Fournaise eruptions are triggered by magma overpressure within a reservoir located below the

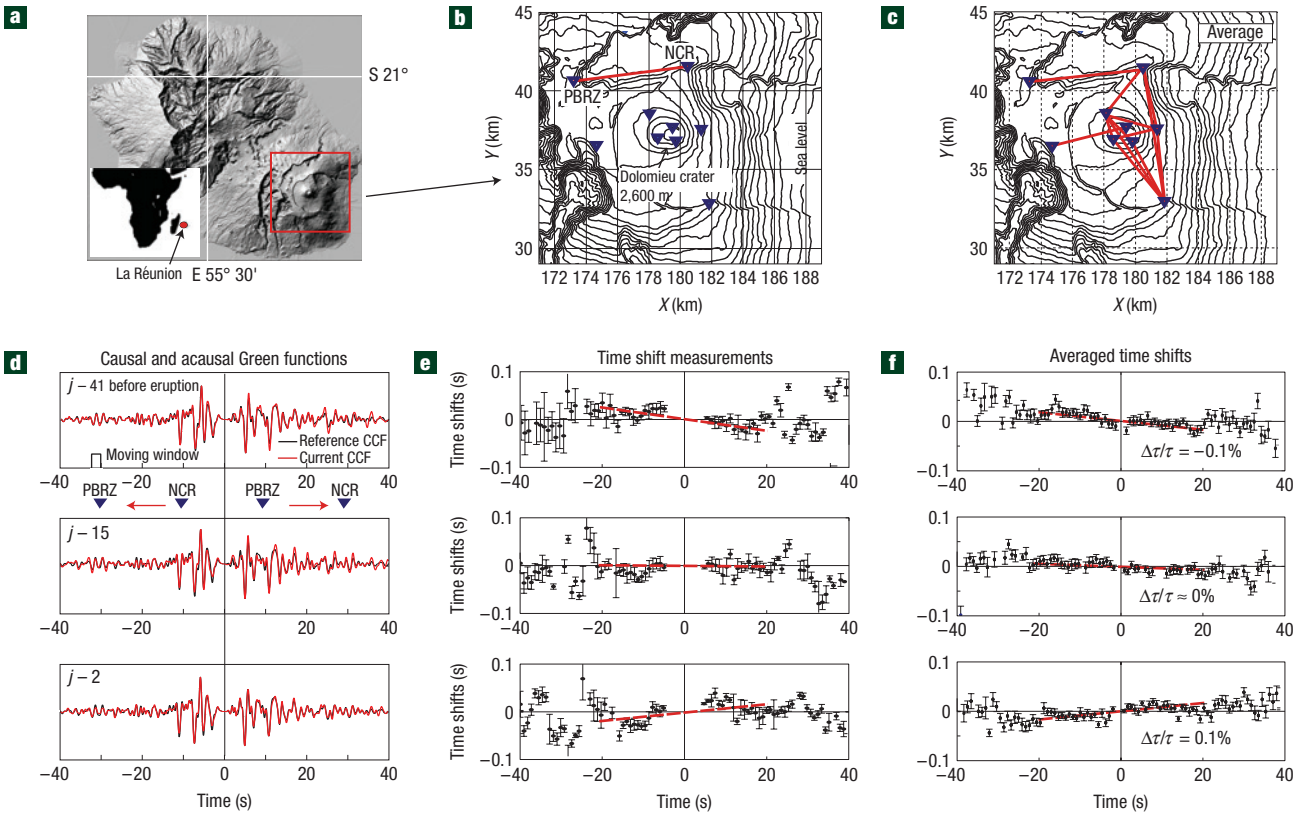

Figure 1 Measurements of relative time perturbations ($\Delta\tau/\tau$). **a**, La Réunion Island. **b**, Topographic map showing a direct path (red line) between two seismic receivers (inverted triangles). **d**, Comparison between filtered ([0.1–0.9] Hz) reference (black curves) and current (red curves) cross-correlation functions (CCF) computed before the eruption of June 2000. **e**, Time shifts and time-shift errors (error bars) measured between the reference and current CCF shown in **d**. Red lines show results of the linear regressions. **f**, Averaged time shifts (using 13 receiver pairs shown in **c**) and resulting measurements of relative time perturbations.

Dolomieu crater (Fig. 1b) at approximately sea level[3,25]. We used the continuous seismic noise recorded between July 1999 and December 2000 by 21 vertical short period receivers operated by the Observatoire Volcanologique du Piton de la Fournaise to compute 210 cross-correlation functions corresponding to all possible receiver pairs[21]. We used the spectral band between 0.1 and 0.9 Hz, where the recovered Green functions have been demonstrated to consist of Rayleigh waves that are sensitive to the structure at depths down to 2 km below the edifice surface. The cross-correlation functions obtained by correlating 18 months of seismic noise are called the reference Green functions (see the Supplementary Information for more detail). The temporal evolution was then tracked by comparing the reference Green functions with current Green functions computed by correlating the noise from a ten-day-long moving window.

If the medium shows a spatially homogeneous relative velocity change $\Delta v/v$, the relative travel-time shift ($\Delta\tau/\tau$) between the perturbed and reference Green functions is independent of the lapse time (τ) at which it is measured and $\Delta v/v = -\Delta\tau/\tau = \text{const}$. Therefore, when computing a local time shift $\Delta\tau$ between the reference and the current cross-correlations in a short window centred at time τ, we would expect to find $\Delta\tau$ to be a linear function of τ (see the Supplementary Information). By measuring the slope of the travel-time shifts $\Delta\tau$ as function of time τ, we finally estimate the relative time perturbation (RTP, $\Delta\tau/\tau$), which is the opposite value of the medium's relative velocity change ($\Delta v/v$). Figure 1d shows the reference and the current Green functions for one pair of receivers (PBRZ–NCR, Fig. 1b) computed 41 days, 15 days and two days before the eruption of June 2000 (day 359). The positive- and negative-time Green functions are normalized separately to highlight the phase symmetry. Figure 1e shows the respective travel-time shifts measured in the frequency band [0.1–0.9] Hz using the moving-window cross-spectrum technique[4] (doublet analysis). It can be seen in these measurements obtained with just one pair of receivers that the RTP changes from a negative to a nearly zero and then to a positive value 41 days, 15 days and two days before the eruption, respectively. The accuracy of the linear trend measurements is significantly improved by averaging local time shifts for different receiver pairs, assuming that the seismic velocities are perturbed uniformly within the sampled medium. We selected 13 receiver pairs located near the caldera and showing good-quality measurements (Fig. 1c) to compute the averaged time shifts (Fig. 1f) and to obtain accurate RTP estimates.

Figure 2a presents the relative velocity changes ($\Delta v/v$) measured over 18 months (June 1999 to December 2000; each relative velocity change measurement is represented at the centre of its associated ten-day-long moving window). Intervals with low-quality measurements that correspond to periods of seismo-volcanic activity (Fig. 2c) and to strong tropical cyclones (days 135–229) are excluded from the analysis (Fig. 2b). The remaining time series indicated that the volcano interior shows changes at different timescales, varying from a few months to a few days. To simplify the analysis, we separate the short- (STV)

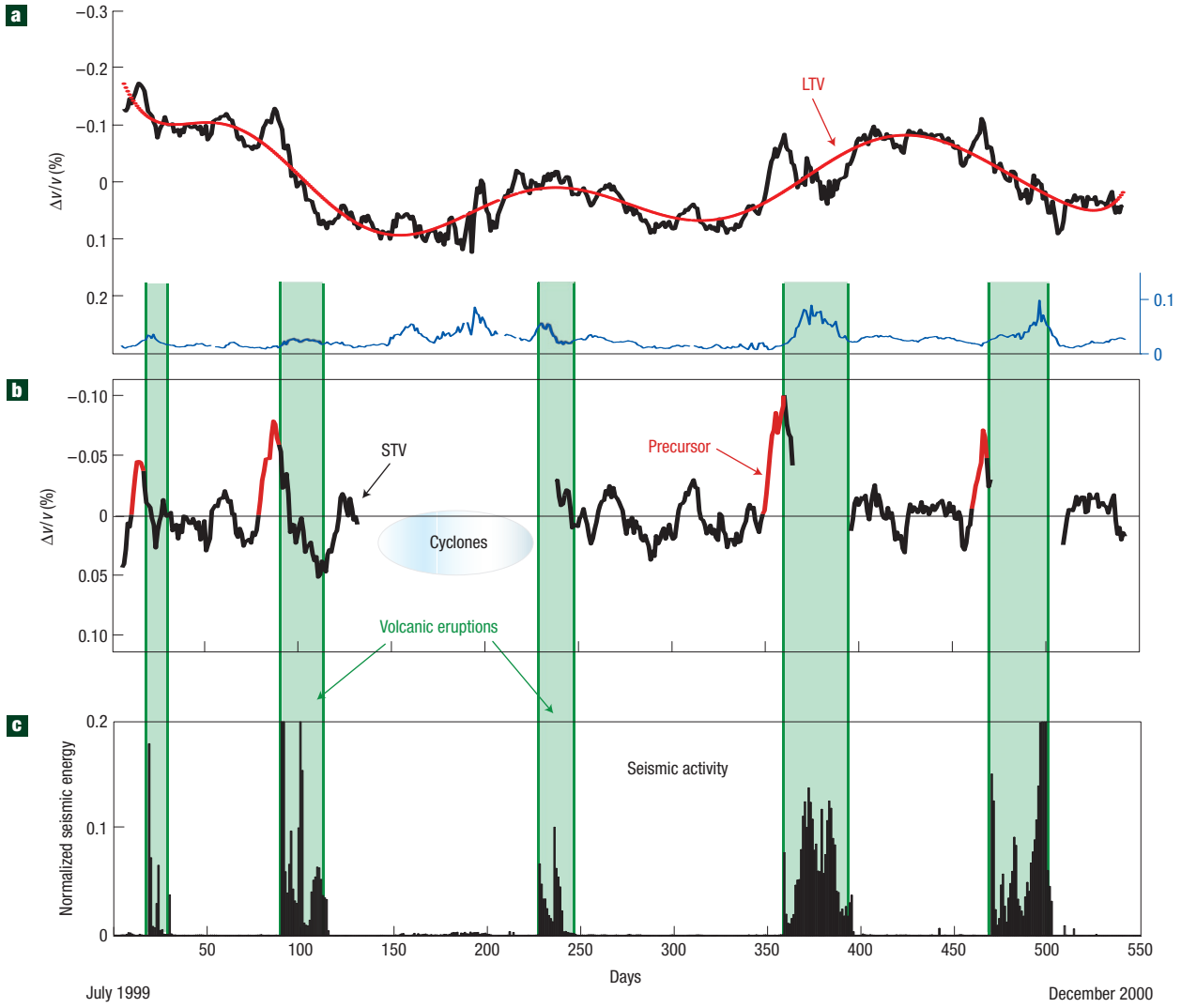

Figure 2 Evolution of relative velocity changes on Piton de la Fournaise over 18 months. a, Raw relative velocity changes over 18 months. The blue error curve represents the uncertainty of the linear slope estimation. Measurements with uncertainties higher than 0.04% are excluded from the analysis. **b**, STV computed as relative velocity changes corrected for the long-term component (LTV). **c**, Daily seismic energy measured by a sensor located near Dolomieu crater.

and the long-term variations (LTV). We fit the raw relative velocity changes by a 11th-order polynomial function to obtain the LTV and then subtract these LTV from the raw relative velocity changes to obtain the STV (Fig. 2b). The short-term variation curve shows clear precursors to the volcanic eruptions characterized by a decrease of seismic velocities. These precursors start about 20 days before the eruptions and correspond to relative velocity changes as small as 0.1%. A discussion concerning the LTV is provided as Supplementary Information.

We interpret the observed short-term decreases in seismic velocities as an effect of the dilatation of a part of the edifice resulting from the magma pressurization (see the Methods section) within the volcano plumbing system, similar to observations at Mount Etna[1]. This interpretation is also supported by the clear opening of an individual fracture detected by an extensometer[26] before eruption n°4 (day 359, June 2000) synchronously with the relative velocity change precursor (see the Supplementary Information). The lack of clear fracture opening precursors for the other eruptions would suggest that the detected dilatation may occur in a restricted zone and have non-measurable effects at the extensometer location. The relative velocity changes return to a nearly background level during the eruption periods (Fig. 2b). This observation is consistent with deflation caused by depressurization of the magma during its extrusion to the surface only a few minutes after the beginning of the eruptions[26]. Other phenomena such as magma migration or heat-flux variations could be evoked to explain the observed velocity variations. However, we believe the proposed hypothesis to be the most plausible.

The relative-velocity-change curve presented in Fig. 2b is an average of the measured time shifts for different receiver pairs located in the vicinity of the main caldera. The same procedure applied to receiver pairs located outside the main caldera does not show eruption precursors. This suggests that the velocity variations are spatially localized. We apply a regionalization procedure to locate more precisely the observed perturbations (see the Supplementary Information). We estimate the relative velocity changes for 28 individual receiver pairs selected according to quality criteria, subtract the long-term component from the

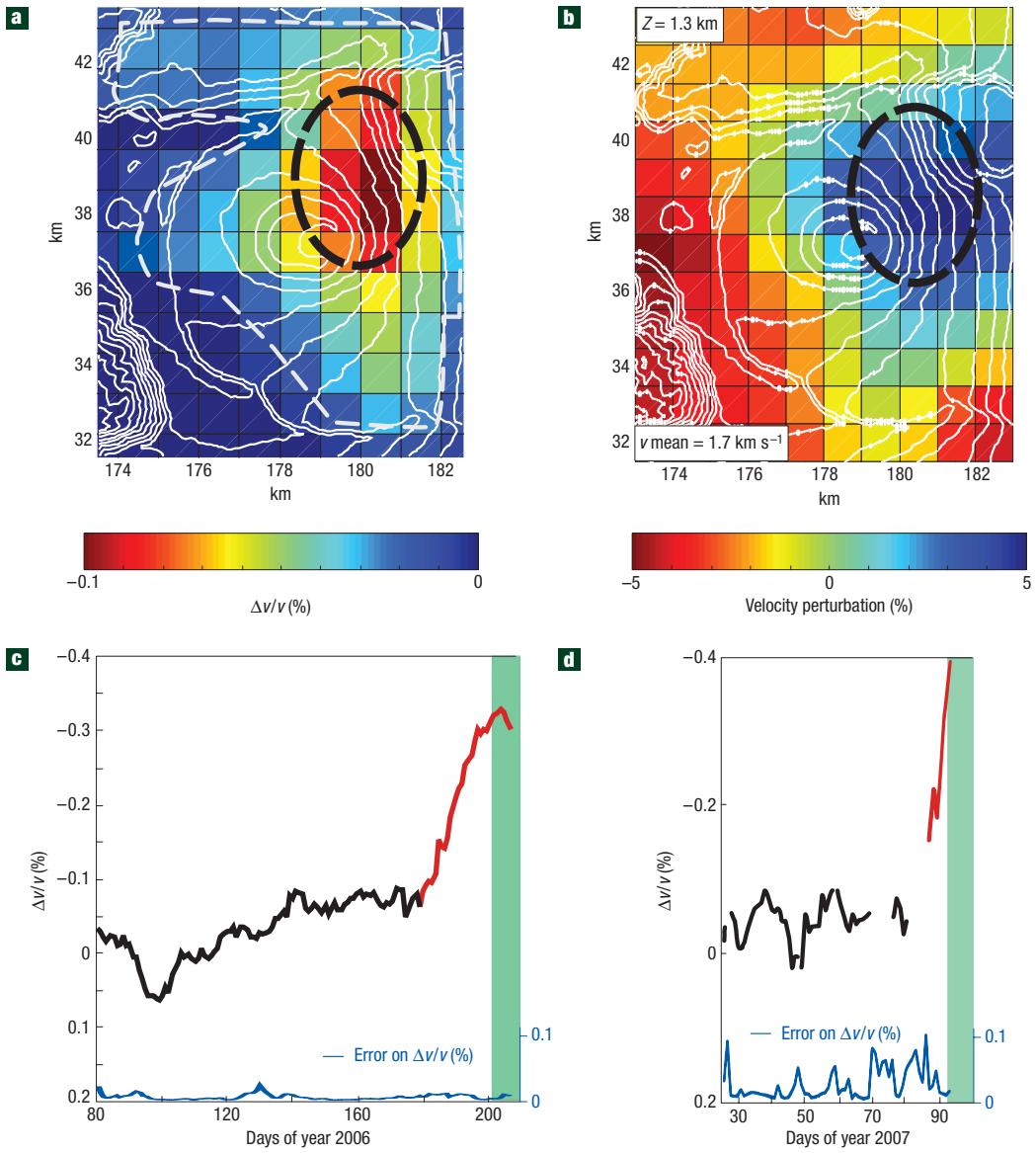

Figure 3 Regionalization of the velocity-variation anomalies. a, Regionalization of the relative velocity changes associated with the second eruption precursor (day 85, September 1999). The white dashed line represents the limits of ray coverage and the black dashed ellipse encloses the location of the relative velocity change anomaly. **b**, High-shear-velocity anomaly (black dashed ellipse) imaged by passive surface-wave tomography[21] and interpreted as an effect of solidified dykes associated with the zone of magma injection. **c**, Relative velocity changes before the eruption of July 2006. **d**, Relative velocity changes before the eruption of April 2007. The strong errors on $\Delta v/v$ are due to cyclonic activity. However, notice that these errors decrease a few days before the eruption.

raw measurements to obtain the STV and then compute, in every grid cell, an average value from its neighbourhood receiver-pair paths. As a result, we obtain for every day a two-dimensional map of relative velocity changes. A full set of these maps is shown in a movie (see the Supplementary Information) and a snapshot taken five days before eruption 2 is presented in Fig. 3a. The movie and snapshot show that the precursors are not distributed homogeneously in space but are mainly located in an area a few kilometres east of the Dolomieu crater. This location nearly coincides with the high-velocity anomaly imaged by surface-wave tomography at 1.3 km above sea level[21] (Fig. 3b) and interpreted as an effect of solidified dykes associated with the zone of magma injection. This coincidence is an additional argument suggesting that the observed short-term seismic velocity decreases are produced by dilatation associated with the pressurization within the volcano plumbing system.

As a pilot experiment, we began monitoring the Piton de la Fournaise volcano by computing in real time the noise cross-correlations and measuring the velocity variations since March 2006. This enabled us to identify clear precursors for the two latest eruptions, which occurred in July 2006 and April 2007 (Fig. 3c,d) and emitted three and 20 times more magma, respectively, than the strongest eruptions of 1999–2000. This is in good agreement with the precursor amplitudes, which are three to four times higher for the two latest eruptions than for the eruptions of 1999–2000. Overall, this new direct observation of the dilatation of volcanic edifices should improve our ability to forecast eruptions and to *a priori* assess their intensity and

environmental impact. Detection of changes in elastic properties on the basis of correlations of seismic noise is a new robust method that may also be useful in other geophysical, engineering and geotechnical applications that require non-destructive monitoring of the media.

METHODS

LINK BETWEEN SEISMIC VELOCITY CHANGES AND MAGMA PRESSURIZATION

The presented measurements are based on Rayleigh waves that dominate the noise cross-correlations. Therefore, the observed travel-time variations mainly correspond to perturbations of shear-wave velocity β. We use empirical laws for porous media[27] to link the relative shear-wave-velocity perturbations to relative perturbations of porosity φ and volume V,

$$-\Delta\tau/\tau = \Delta\beta/\beta = -1/2 \times \Delta\varphi/\varphi = -1/2 \times \Delta V/(V \times \varphi),$$

which can be, in turn, related to the overpressure ΔP induced in the medium by the magma using a model of dilatancy:

$$\Delta V/V = \Delta P/K,$$

where K is the incompressibility factor of the medium, which can be estimated as approximately 10 GPa by considering an average P-wave speed of 3,400 m s^{-1}, a density of 2,000 kg m^{-3} and a shear modulus value of 10 GPa. We then take $\Delta\beta/\beta = -1 \times 10^{-3}$ and an average realistic porosity of 0.1 and find ΔP to be approximately equal to 2 MPa or 20 bar. This overpressure level is consistent with theoretical and experimental models of dyke migration[28,29] and with recent interpretation of strain data on the Soufrière Hills volcano of Montserrat[30] as well as with the model of dyke propagation developed to explain the geodetic observations on Piton de la Fournaise[26].

Received 5 June 2007; accepted 23 November 2007; published 20 January 2008.

References

1. Patanè, D., De Gori, P., Chiarabba, C. & Bonaccorso, A. Magma ascent and the pressurization of Mount Etna's volcanic system. *Science* **299**, 2061–2063 (2003).
2. Massonnet, D., Briole, P. & Arnaud, A. Deflation of Mount Etna monitored by spaceborne radar interferometry. *Nature* **375**, 567–570 (2001).
3. Peltier, A., Ferrazzini, V., Staudacher, T. & Bachèlery, P. Imaging the dynamics of dyke propagation prior to the 2000–2003 flank eruptions at Piton de La Fournaise, Reunion Island. *Geophys. Res. Lett.* **32**, L22302 (2005).
4. Ratdomopurbo, A. & Poupinet, G. Monitoring a temporal change of seismic velocity in a volcano: Application to the 1992 eruption of Mt. Merapi (Indonesia). *Geophys. Res. Lett.* **22**, 775–778 (1995).
5. Snieder, R. & Hagerty, M. Monitoring change in volcanic interiors using coda wave interferometry: Application to Arenal Volcano, Costa Rica. *Geophys. Res. Lett.* **31**, L09608 (2004).
6. Battaglia, J., Ferrazzini, V., Staudacher, T., Aki, K. & Cheminée, J.-L. Pre-eruptive migration of earthquakes at the Piton de la Fournaise volcano (Réunion Island). *Geophys. J. Int.* **161**, 549–558 (2005).
7. Chouet, B. Long-period volcano seismicity: Its source and use in eruption forecasting. *Nature* **380**, 309–316 (1996).
8. Chouet, B. Volcano seismology. *Pure Appl. Geophys.* **160**, 739–788 (2003).
9. Poupinet, G., Ellsworth, W. L. & Frechet, J. Monitoring velocity variations in the crust using earthquake doublets: An application to the Calaveras Fault, California. *J. Geophys. Res.* **89**, 5719–5731 (1984).
10. Wegler, U., Lühr, B.-G., Snieder, R. & Ratdomopurbo, A. Increase of shear wave velocity before the 1998 eruption of Merapi volcano (Indonesia). *Geophys. Res. Lett.* **33**, L09303 (2006).
11. Grêt, A., Snieder, R., Aster, R. C. & Kyle, P. R. Monitoring rapid temporal change in a volcano with coda wave interferometry. *Geophys. Res. Lett.* **32**, L06304 (2005).
12. Sabra, K. G., Roux, P., Gerstoft, P., Kuperman, W. A. & Fehler, M. C. Extracting coherent coda arrivals from cross-correlations of long period seismic waves during the Mount St. Helens 2004 eruption. *Geophys. Res. Lett.* **33**, L06313 (2006).
13. Patanè, D., Barberi, G., Cocina, O., De Gori, P. & Chiarabba, C. Time-resolved seismic tomography detects magma intrusions at Mount Etna. *Science* **313**, 821–823 (2006).
14. Weaver, R. L. & Lobkis, O. I. Ultrasonics without a source: Thermal fluctuation correlations at MHz frequencies. *Phys. Rev. Lett.* **87**, 134301–134304 (2001).
15. Campillo, M. & Paul, A. Long-range correlations in the diffuse seismic coda. *Science* **299**, 547–549 (2003).
16. Shapiro, N. M. & Campillo, M. Emergence of broadband Rayleigh waves from correlations of the ambient seismic noise. *Geophys. Res. Lett.* **31**, L07614 (2004).
17. Sabra, K. G., Gerstoft, P., Roux, P., Kuperman, W. A. & Fehler, M. C. Extracting timedomain Green's function estimates from ambient seismic noise. *Geophys. Res. Lett.* **32**, L03310 (2005).
18. Campillo, M. Phase and correlation in random seismic fields and the reconstruction of the Green function. *Pure Appl. Geophys.* **163**, 475–502 (2006).
19. Shapiro, N., Campillo, M., Stehly, L. & Ritzwoller, M. H. High-resolution surface-wave tomography from ambient seismic noise. *Science* **307**, 1615–1618 (2005).
20. Sabra, K. G., Gerstoft, P., Roux, P., Kuperman, W. A. & Fehler, M. C. Surface wave tomography from microseisms in Southern California. *Geophys. Res. Lett.* **32**, L14311 (2005).
21. Brenguier, F., Shapiro, N. M., Campillo, M., Nercessian, A. & Ferrazzini, V. 3D surface wave tomography of the Piton de la Fournaise volcano using seismic noise correlations. *Geophys. Res. Lett.* **34**, L02305 (2007).
22. Stehly, L., Campillo, M. & Shapiro, N. M. Travel time measurements from noise correlation: Stability and detection of instrumental errors. *Geophys. J. Int.* **171**, 223–230 (2007).
23. Sens-Schönfelder, C. & Wegler, U. Passive image interferometry and seasonal variations of seismic velocities at Merapi Volcano, Indonesia. *Geophys. Res. Lett.* **33**, L21302 (2006).
24. Stieltjes, L. & Moutou, P. A statistical and probabilistic study of the historic activity of the Piton de la Fournaise, Réunion Island, Indian Ocean. *J. Volcanol. Geotherm. Res.* **36**, 67–86 (1989).
25. Nercessian, A., Hirn, A., Lépine, J.-C. & Sapin, M. Internal structure of Piton de la Fournaise volcano from seismic wave propagation and earthquake distribution. *J. Volcanol. Geotherm. Res.* **70**, 123–143 (1996).
26. Peltier, A. *et al*. Subtle precursors of volcanic eruptions at Piton de la Fournaise detected by extensometers. *Geophys. Res. Lett.* **33**, L06315 (2006).
27. Pride, S. R. *Hydrogeophysics* Ch. 8, 253–290 (Water Science and Technology Library, Springer, Berlin, 2005).
28. Tait, S., Jaupart, C. & Vergniolle, S. Pressure, gas content and eruption periodicity of a shallow crystallising magma chamber. *Earth Planet. Sci. Lett.* **92**, 107–123 (1989).
29. McLeod, P. & Tait, S. The growth of dykes from magma chambers. *J. Volcanol. Geotherm. Res.* **92**, 231–245 (1999).
30. Voight, B. *et al*. Unprecedented pressure increase in deep magma reservoir triggered by lava-dome collapse. *Geophys. Res. Lett.* **33**, L03312 (2006).

Acknowledgements

All the data used in this work were collected by the seismological network of the Observatoire Volcanologique du Piton de la Fournaise. We are grateful to the Observatory staff. We thank L. Stehly, P. Gouédard, L. de Barros, E. Larose, P. Roux and C. Sens-Schönfelder for helpful discussions. We are grateful to A. Peltier and Meteo France for providing us with extensometer and meteorological data respectively. We thank F. Renard, I. Manighetti and G. Poupinet for constructive comments concerning the manuscript. This work was supported by ANR (France) under contracts 05-CATT-010-01 (PRECORSIS) and ANR-06-CEXC-005 (COHERSIS).
Correspondence and requests for materials should be addressed to F.B.
Supplementary Information accompanies this paper on www.nature.com/naturegeoscience.

Author contributions

F.B., N.M.S., M.C. and Z.D. carried out the data analysis. M.C. was also the project manager. Z.D. also carried out field work. V.F. and A.N. were responsible for preliminary tests and data collection. O.C. carried out the computer code programming.